Zirconium Oxo Cluster Catalyzed Dipeptide Cyclization Evaluated by Experiments and Theory

Alexander Peeters,[1] Jordi Puiggalí-Jou,[2] Yujie Zhang,[1] Ismail Y. Kokculer,[1] Albert Solé-Daura,[2,3] Jorge J. Carbó,[2,*] Tatjana N. Parac-Vogt[1,*] and Francisco de Azambuja[1,*]

[1] Department of Chemistry, KU Leuven, Celestijnenlaan 200F, 3001 Leuven, Belgium

[2] Departament de Química Física i Inorgànica, Universitat Rovira i Virgili, Marcel·lí Domingo, 1, 43007 Tarragona, Spain.

[3] Institute of Chemical Research of Catalonia (ICIQ-CERCA), The Barcelona Institute of Science and Technology, Avgda. Països Catalans, 16, 43007 Tarragona, Spain.

* francisco.deazambuja@kuleuven.be, tatjana.vogt@kuleuven.be, j.carbo@urv.cat

Abstract. Although peptides are essential for many areas of chemistry, key limitations still remain to their synthesis, such as high costs and poor atom-economy. An ideal alternative is the catalytic peptide bond formation directly from non-activated amino acids; however, the high-energy barrier associated with this reaction hampers the development of suitable alternatives. In this work, we evaluated the catalytic activity of discrete zirconium oxo clusters for direct peptide bond formation, using dipeptide cyclization as model reaction. The clusters afforded several 2,5-diketopiperazine derivatives in good to excellent yields under straightforward open-flask conditions, without requiring the water by-product to be scavenged from the reaction. Further mechanistic study through Density Functional Theory (DFT) calculations revealed that the mechanism involves a second substrate molecule near the reactive site of the catalysts, to streamline proton transfers that push the reaction forward. These results underline the promising potential of discrete ZrOCs as an emerging class of catalysts for the formation of peptide bonds under green, straightforward reaction conditions.

Keywords: zirconium, zirconium oxo clusters, metal oxo clusters, peptides, peptide bond formation, cyclization, mechanism, DFT

Introduction

The discovery of solid-phase peptide synthesis (SPPS) allowed the chemical synthesis of practically any peptide envisioned.[1-2] However, this method has multiple downsides: i) it uses stoichiometric activating agents and large volumes of solvent, resulting in a poor atom economy; ii) excessive reliance on dimethylformamide (DMF) as a solvent,[3] which is restricted in production environments by the European Union due to its toxicity;[4] iii) the explosive and allergy-inducing nature of commonly used carboxyl-activating benzotriazoles (TBTU, HBTU, HATU…).[5-6] These downsides were also pointed out by the American Chemical Society Green Chemistry Institute (ACS GCI), the industry-academia forum in the United States.[7]

A key strategy to reduce the environmental impact of peptide synthesis is to catalyze the direct amide bond formation, generating only water as a by-product.[8-11] However, the majority of catalysts reported so far require the removal of water to work optimally, which sharply decreases the atom economy and increases the energy consumption of these methods[12] and hinders their widespread industrial use.[13-14] Recently, we have demonstrated that metal oxo clusters[15-17] are promising viable candidates for the catalytic synthesis of amides due to their resilience to the presence of large amounts of water.[18-20] In addition, we have shown that metal oxo clusters play a key role in the reactivity even when starting with commercially available precursors, which enables the synthesis of amides without water scavenging.[21] Intrigued by this highly promising prospect, we turned to the development of a catalytic peptide bond formation reaction. This reaction is not only useful for the synthesis of linear peptides, but also contributes to the synthesis of natural products, and increasingly attractive (cyclic) bioactive peptide compounds.[22] In particular, diketopiperazines derived from the cyclization of dipeptides are of high interest due to their scaffold being present in a broad range of natural products.[23]

Metal catalysis with elements of group IV and V has been previously studied for the direct amidation reaction.[9, 24-25] Recently, some notable advances have been reported such as the tantalum and titanium-based catalysts, which directly form peptide bonds through a 7-membered ring transition state that prevents epimerization.[24] Meanwhile, zirconium-based catalysts remain interesting candidates for these reactions because of zirconium large availability as a byproduct from titanium and tin mining[13,14] and their good stability under various reaction conditions. In this work, we developed the reactivity of zirconium oxo clusters (ZrOCs)[15, 26-27] towards the direct amidation of peptides by studying the intramolecular cyclization of unprotected, readily available dipeptides by means of experimental and computational tools. The discrete ZrOCs clusters catalyze the formation of peptide bonds in good to excellent yields under green, straightforward reaction conditions, underlining the promising potential of this emerging class of catalysts.

Results and discussion

To probe the ability of ZrOCs to catalyze the formation of peptide bonds, the cyclization of glycylglycine (**1a**) to 2,5-diketopiperazine (**2a**) was evaluated upon incubation of **1a** with different zirconium oxo clusters (ZrOCs, Figure 1). After an initial solvent screening (Table S1), we identified DMSO as the most efficient reaction medium. Thus, we used this solvent to probe the reactivity of different Zr oxo clusters (Table 1).

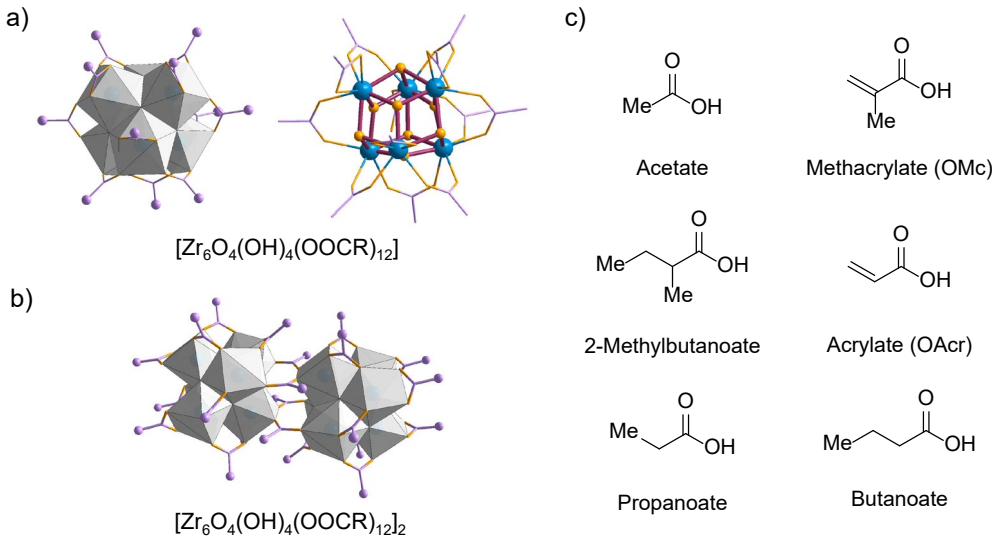

Figure 1. Representative structures of the a) hexanuclear and b) dodecanuclear Zr oxo cluster (ZrOC) used in this study using a combination of polyhedron, wires/sticks and ball-and-stick models. Grey polyhedrons represent {Zr_6O_8}, blue zirconium, light purple carbons, and gold yellow oxygens. c) Structure of carboxylate ligands present in the ZrOC used in this work.

Table 1. Zr oxo clusters afford diketopiperazine **2a**

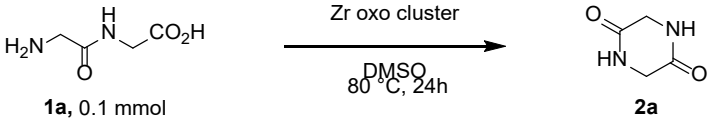

1a, 0.1 mmol **2a**

Entry[a]	Catalyst	Ligand	Yield **2a** (%)[b]
1	**Zr_6-OMc**	Methacrylate	23
2	**Zr_6-OAc**	Acetate	45
3	**Zr_6-2-Me-butanoate**	2-Methylbutanoate	28
4	**Zr_{12}-OAcr**	Acrylate	2
5	**Zr_{12}-OAc**	Acetate	99
6	**Zr_{12}-Propanoate**	Propanoate	91
7	**Zr_{12}-Butanoate**	Butanoate	59

[a] Reaction condition: Gly-Gly (0.100 mmol), solvent (1.00 mL), Zr oxo clusters (2.5 mol%), 80 °C, 24 h. [b] ^{1}H NMR yields.

After identifying the most prominent reactivities, we underwent a comprehesive optimization of the reaction conditions varying the temperature, catalyst loading and reaction time. Representative results are given in Table 2 for **Zr_{12}-Butanoate** (complete results in the SI). In general, we observed that increasing temperature, catalyst loading and reaction time led to an increase of yield in different extents. Most notably, the temperature caused a more significant difference. That is, reactions at 80 °C generally did not afford the same efficiency as reactions conducted at 100 °C, even with higher catalyst loading and/or long reaction times.

Optimization in MeOH/EtOH

Considering our previous results showed that the peptide bond formation can be achieved in MeOH or EtOH using Zr_6-containing MOFs,[20] and the favorable green profile of EtOH, we decided to build up on the reactivity observed in DMSO and investigate the reactivity of these clusters in alcoholic solvents. For this study, we started our exploration by probing a Zr_6 and a Zr_{12} cluster. For the Zr_6 cluster, we chose **Zr_6-OMc** as this discrete cluster exhibited good catalytic reactivity for the intermolecular amide bond formation between phenylacetic acid and benzylamine in ethanol, which gives precedent for potential efficient peptide bond formation.[18] For the Zr_{12} cluster, we used **Zr_{12}-Butanoate** as a representative example due to its good solubility in alcoholic solvents.

Table 2. Optimization of the reaction conditions for the GlyGly cyclization reaction in different alcohols.

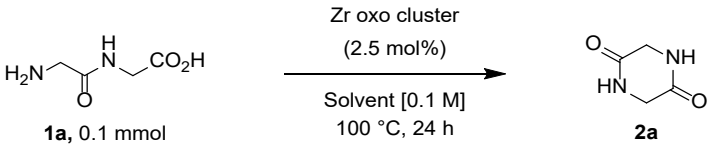

1a, 0.1 mmol — **2a**

Entry[a]	Catalyst	Solvent	Yield **2a** (%)[a]
1	**Zr_6-OMc**	DMSO	95
2	**Zr_6-OMc**	MeOH	24
3	**Zr_{12}-Butanoate**	DMSO	99
4	**Zr_{12}-Butanoate**	MeOH	37
5	**Zr_{12}-Butanoate**	EtOH	87
6	**Zr_{12}-Butanoate**	^{n}PrOH	13

[a] ^{1}H NMR yields.

In general, the reactivity in alcoholic solvents was better at 100 °C (Table S4 – S6), and good yields for the cyclization of **1a** could be observed even using a low 2.5 mol% loading of the catalysts (Table 2). Attempts to optimize **1a** cyclization reaction using EtOH as a solvent at 80 °C by changing the global concentration of the reaction, nature of cluster catalyst used and reaction time were unsuccessful (Table S6). Additionally, using dry conditions, or first stirring the reaction at 100 °C for 1 hour to induce a ligand exchange with the substrate prior to carrying out the reaction at 80 °C were also not fruitful (Table S6). Finally, using mixtures of EtOH and DMSO as a solvent was also ineffective to improve the reactivity (Table S7). Although the reactivity in alcoholic solvents is more challenging and require high temperature to afford good yields, these results show that the reactivity in these solvents can be drastically improved by the nature of ligands surrounding the catalytic active cluster core.

Reaction scope

Other peptides and amino acid substrates were also cyclized in the presence of ZrOCs showing the intramolecular bond formation observed is not limited to GlyGly (**Table 3**). Moreover, several substrates could be cyclized using ethanol as solvent, showcasing the compatibility of these catalysts with a green solvent (Table 3, entries 1-7). Using substrates other than GlyGly, the cyclized products were generally observed in good to

excellent yield for the serine (entry 1), alanine (entries 2 and 3), proline (entries 4 and 5), leucine (entry 6), phenylalanine (entry 7) histidine (entry 8), and aspartic acid (entry 9) containing dipeptides, demonstrating the compatibility of this catalytic system with functional groups widely present in drug candidates and biomolecules.[20] Comparable good yields were also observed when X-Gly peptide were used (entries 3 and 5), showcasing that the presence of substituents next to the nucleophilic amino group are also tolerated. Further, the cyclization of Ala-Ala showed that the reaction was not limited to glycine containing dipeptides (Entry 10). Moreover, the high yield provided with a reaction time of 144h highlights that the catalyst was not deactivated by side processes even after considerably long reaction time. Careful analysis of the crude reaction mixture of **2i** also evidence the absence of diastereoisomers, indicating this cyclization occurs without noticeable epimerization, which is consistent with other Zr-catalyzed amide bond formation reactions previously reported.[18, 20, 28-29] Finally, the high yield of cyclic products provided by nonpeptide substrates γ-aminobutyric acid and its homologue 5-aminovaleric acid (Entry 11) showed that the formation of the reaction is not limited to diketopiperazines or products that contain six-membered rings.

Table 3. Reaction scope

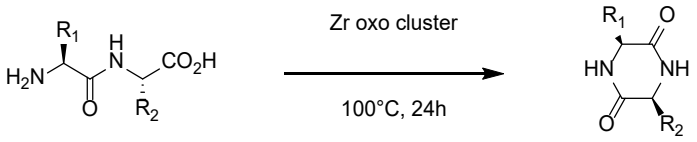

1b-k **2b-2k**

Entry	Substrate	Product	Catalyst	mol%	Solvent	Yield **2a** (%)[b]
1	H-Gly-Ser-OH	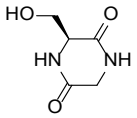 **2b**	**Zr_6-OMc**	10.0	DMSO	76
			Zr_{12}-Butanoate	2.5	DMSO	99
			Zr_{12}-Butanoate	2.5	EtOH	77
2	H-Gly-Ala-OH	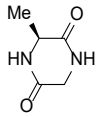 **2c**	**Zr_6-OMc**	10.0	DMSO	75
			Zr_{12}-Butanoate	2.5	DMSO	99
			Zr_{12}-Butanoate	2.5	EtOH	99
3	H-Ala-Gly-OH	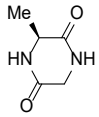 **2c**	**Zr_6-OMc**	2.5	DMSO	99
			Zr_{12}-Butanoate	2.5	EtOH	99
4	H-Gly-Pro-OH	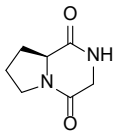 **2d**	**Zr_6-OMc**	10.0	DMSO	58
			Zr_{12}-Butanoate	2.5	DMSO	99
			Zr_{12}-Butanoate	2.5	EtOH	94

5	H-Pro-Gly-OH	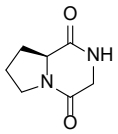 **2d**	**Zr_{12}-Butanoate**	2.5	DMSO	99
			Zr_{12}-Butanoate	2.5	EtOH	96
6	H-Gly-Leu-OH	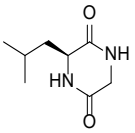 **2e**	**Zr_{12}-Butanoate**	2.5	DMSO	75
			Zr_{12}-Butanoate	2.5	EtOH	99
7	H-Gly-Phe-OH	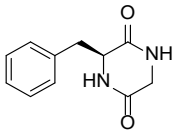 **2f**	**Zr_{12}-Butanoate**	2.5	DMSO	99
			Zr_{12}-Butanoate	2.5	EtOH	93
8	H-Gly-His-OH	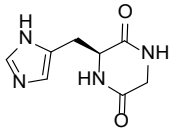 **2g**	**Zr_6-OMc**	2.5	DMSO	74
9	H-Gly-Asp-OH	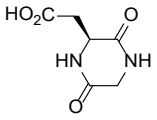 **2h**	**Zr_6-OMc**	2.5	DMSO	53
10[c]	H-Ala-Ala-OH	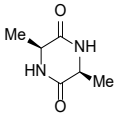 **2i**	**Zr_6-OMc**	10.0	DMSO	78
11	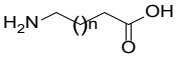	 **2j-l**	**Zr_6-OMc**	10.0	DMSO	99 (n = 1) 99 (n = 2)

[a] Reaction condition: **1a** (0.100 mmol), solvent (1.00 mL), **Zr oxo cluster** (2.5 – 10.0 mol%), 100 °C, 24 h. [b] ^{1}H NMR yields. [c] 144 h.

Considering the promising reaction scope for the intramolecular reaction (Table 3), we have also probed a preliminary experiment aiming at the highly desired direct intermolecular peptide bond formation[1] by attempting the formation of GlyGly substrate (**1a**) or its corresponding cyclization product **2a** directly from commercially available non-protected glycine under similar conditions. Given the more challenging nature of this reaction, we

directly used anhydrous reactions conditions and a higher catalyst loading than the typical 2.5 mol% employed in Table 3 (Scheme 1). Remarkably, cyclic GlyGly (**1a**) was obtained in 51% yield, showcasing the ability of these novel discrete catalysts to form both *inter-* and intramolecular peptide bonds with synthetically useful efficiency in a single reaction step.

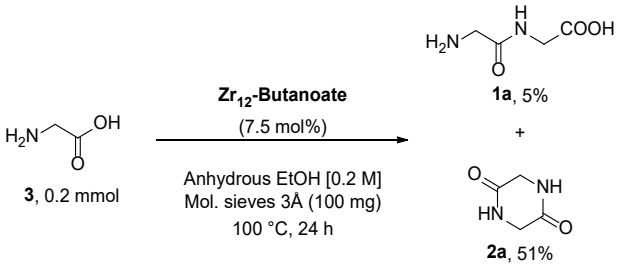

Scheme 1. Proof-of-concept of intermolecular peptide bond formation by Zr oxo cluster catalysis in EtOH

Computational Study

The experimental results discussed above showcase the promising potential of ZrOCs as catalysts for peptide bond formation. However, we remained intrigued by the harsh reaction conditions required to observe good yields. In our previous work, amide bond formation occurred smoothly at 70 – 80 °C in various solvents.[21, 30-31] Meanwhile, the dipeptide cyclization reported here consistently requires 100 °C to afford good yields. Thus, we turned to DFT calculations to gain deeper mechanistic insights into the intramolecular dipeptide cyclization catalyzed by ZrOCs. Specifically, we focused on the glycylglycine (**1a**) cyclization into **2a** promoted by **Zr_6-OMc** in DMSO at 100 °C as a model reaction. Under these conditions, the reaction showed efficiency and robustness, enabling high yields for different dipeptide substrates (see Table 2 and 3) and thus, it is representative of ZrOCs' reactivity towards dipeptide cyclization. Based on the characterized mechanism for intermolecular amide formation by **Zr_6-OMc** cluster,[21] and dipeptide cyclization by a Zr-MOF,[20] we initially proposed a catalytic cycle for the formation of cyclic product **2a** consisting of five main steps: 1) ligand exchange, whereby the substrate binds to the ZrOC catalyst; 2) C—N bond formation upon nucleophilic attack of the terminal amine to the carboxylate carbon; 3) substrate-assisted N-to-O proton shift in the as-formed zwitterionic intermediate; 4) cleavage of the C—O bond; and 5) regeneration of the active form of the catalyst via substrate-by-product exchange, releasing a water molecule.

Our previous work showed that the initial ligand exchange process occurs through an associative amine-assisted mechanism as illustrated in Figure 2.[21] The most labile methacrylate ligand, which highlighted in green, is replaced by the dipeptide substrate that coordinates to the Zr oxo core through the terminal carboxylate group bridging two neighboring Zr centers yielding the catalytic active species **A**. Its formation involves a proton transfer from substrate (**1a**) to methacrylate ligand, resulting in the release of methacrylic acid (McH); the formation of an intramolecular hydrogen bond between the amino group of **1a** and the a protonated oxo group of the cluster; and the coordination of an additional neutral dipeptide substrate to a Zr site through its amino group (Figure 2). Structurally, amine coordination to Zr induces a marked elongation of the *trans* μ_3-OH bond in

A, consistent with the preference of Zr(IV) for an effective coordination number of eight (Figure S2a).[32-33] As discussed previously,[21] amine binding can promote conversion of substrate's carboxylate group from η^2- to η^1-coordination (from **A** to **Aη^1**), incurring a small free-energy penalty of 1.3 kcal mol^{-1}, which indicates that both species can coexist under catalytic conditions. However, species **Aη^1** bears a less electrophilic carboxylate group since it is activated by the Lewis acidity of only one Zr center. Thus, it can be regarded as an off-cycle species, whose formation does not interfere in the reaction mechanism.

This whole ligand exchange process was calculated to be exergonic by 21.8 kcal·mol^{-1}, and based on previous works,[21, 34-37] we can assume that ligand exchange proceeds smoothly through low free-energy barriers and is not expected to be the rate-determining step in the catalytic cycle. Moreover, the ligand exchange could involve different sites of the catalyst and stages of the catalytic process, as well as replacement of several methacrylate ligands in the same cluster, resulting in complex configurational scenario. However, the various possible configurations are not expected to modify significantly the catalytic features of the Zr_6 cluster. For example, the NBO atomic charge of the coordinated carboxylate carbon in **A** (+ 0.90 *e*), which receives the nucleophilic attack of the amine group, does not vary upon exchanging a second methacrylate ligand by substrate **1a**. Thus, for the sake of computational efficiency, methacrylate ligands at remote positions from the reactive sites were replaced by smaller formate ligands. Such simplification was successfully adopted previously, as it does not to have significant impact on the structural and electronic features of the catalyst.[21, 38]

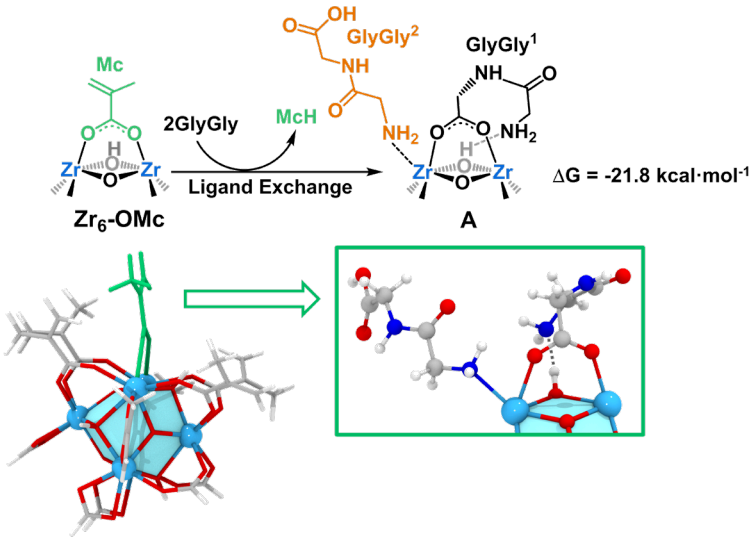

Figure 2. Schematic representation of the catalytic active species **A**, shown with the 3-D structures of the **Zr_6-OMc** model and species **A** which is zoomed in the bi-metallic Zr-Zr centers where the reactivity has been studied according to the employed model. Color code: light blue (Zr), dark blue (N), red (O), gray (C) and white (H). McH = methacrylic acid.

The free-energy profile for the cyclization process starting from species **A**, which binds two GlyGly (**1a**) molecules in distinct coordination modes, is outlined in Figures 3 and 4. First, the terminal amino group of the GlyGly molecule bound to two Zr centers performs an intramolecular nucleophilic attack to its carboxylate group,

which is being activated by the Lewis acid Zr(IV) sites. This takes place through the transition state **TS_{AB}**, represented in Figure S2b, and yields zwitterionic intermediate **B** displaying a new C–N bond. The free-energy barrier associated with this step was found to be 13.7 kcal·mol^{-1}. Interestingly, a similar reaction **A** to **B** without the coordination of the additional dipeptide was also energetically feasible (Figure S3), but it shifted up in energy with respect to the amine-assisted one in Figure 3. Furthermore, an analogous intermolecular reaction through transition state **TS_{AB}'** (Figure S4) would require additional 6.5 kcal·mol^{-1} than **TS_{AB}** due to the entropic penalty. This energetic scenario is consistent with experiments and supports the preference for the intramolecular reaction in Figure 3 rather than intermolecular coupling of two dipeptide molecules. The role of Zr(IV) sites in ZrOCs catalyst as Lewis acidic centers in this step is evident from the energy of the Lowest Unoccupied Molecular Orbitals (LUMO) hosting the π*-type orbital centered on the carboxylate carbon, which lowers from +0.68 to +0.38 eV upon coordination to zirconium (Figure S5). Such energy lowering relates directly on the carboxylate electrophilicity, and thus, it correlates with the feasibility of the nucleophilic attack.[39-41]

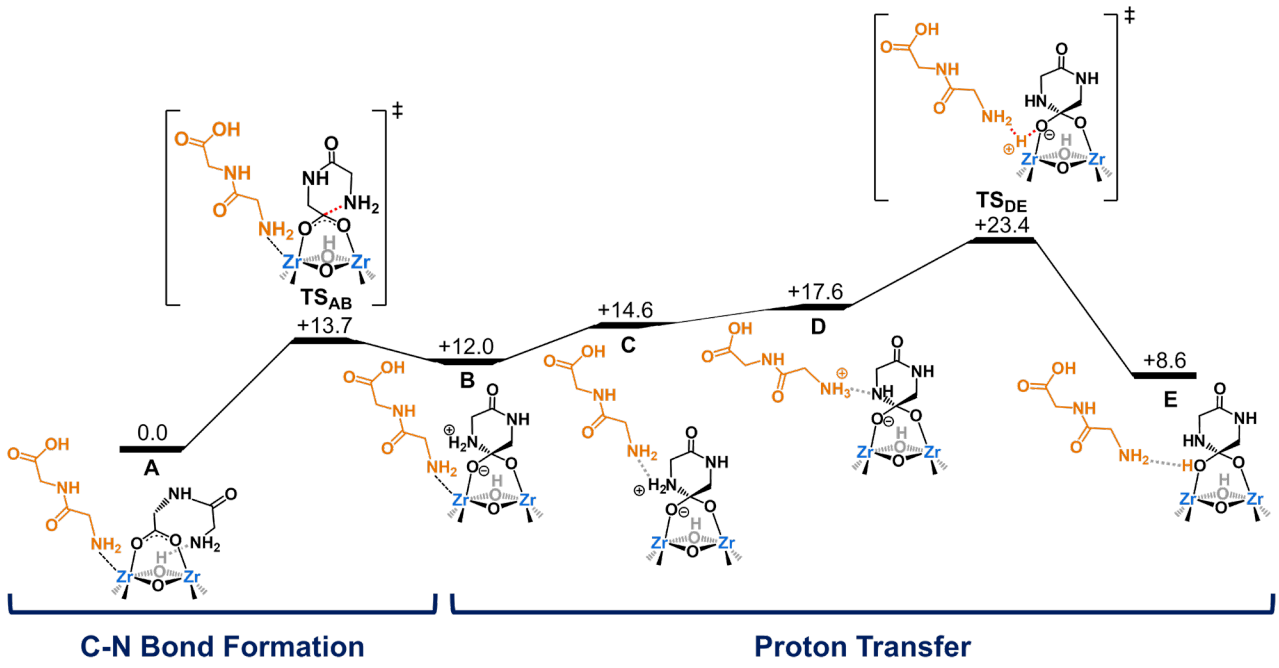

Figure 3. Calculated Gibbs free-energy profile for the C—N bond formation and proton transfer steps involved in the cyclization of **GlyGly** catalyzed by **Zr_6-OMc**. All relative free energies are referred to **A** and are displayed in kcal·mol^{-1}.

The zwitterionic intermediate **B** lies 12.0 kcal·mol^{-1} above **A**, representing a shallow intermediate that can evolve toward species **E** via proton transfer from the positively charged ammonium group to one of the negatively charged Zr-bound oxygen atoms of the substrate. As shown in Figure 3, this transformation proceeds through a stepwise mechanism mediated by the amino group of the substrate molecule initially coordinated to one of the Zr centers though the N atom (represented in orange). The reaction progresses in an overall uphill manner from **A** to **TS_{DE}** (Figure 3), whereas the proton transfer from **C** to **D** proceeds with a very small free-energy

barrier via $\mathbf{TS_{CD}}$ (see Figure S6 and S7 for details). Consequently, the formation of **E** requires overcoming a moderate, yet still accessible, overall barrier of 23.4 kcal·mol^{-1}, which was identified as the rate-determining barrier of the whole catalytic cycle. Notably, this mechanism diverges at the proton-transfer step from other mechanistic studies of this type of reaction involving Zr-MOFs, which share fundamental aspects with ZrOCs.[20] Previously, it was proposed that ethanol solvent molecules participate explicitly in the reaction acting as proton shuttles. Specifically, deprotonation of ethanol molecules on the nodes of Zr-MOFs leads to Zr-bound alkoxide groups that are readily available for mediating the proton-transfer step.[38] In contrast, our results indicate that ZrOCs can indeed operate in aprotic solvent such as DMSO, where proton transfers can be entirely mediated by substrate molecules, thereby offering new mechanistic insights into Zr-catalyzed dipeptide cyclization processes. Note that direct N-to-O proton transfer without the assistance of a second substrate molecule proceeds through a strained, 4-membered ring transition state, which is significantly less stable than those involved in the assisted mechanism presented in Figure 3.[18]

Subsequent steps toward the formation of the product **2a** and regeneration of the catalyst are shown in the reaction profile of Figure 4. Species **E**, which remains 8.6 kcal·mol^{-1} less stable than **A**, undergoes C—O(H) bond cleavage via $\mathbf{TS_{EF}}$ (see Figure S8), overcoming a low free-energy barrier of 3.8 kcal·mol^{-1}. This leads to intermediate **F**, in which the products of the C—O bond cleavage (i.e. a hydroxyl group and a product **2a** molecule) remain coordinated to the Zr centers of the catalytic site. Notably, such a bond cleavage with concomitant formation of the carbonyl group is highly stabilizing, placing **F** 6.6 kcal·mol^{-1} below **A** in terms of free-energy, and thus rendering the whole process effectively irreversible, with a reverse barrier of 30 kcal·mol^{-1} from **F** to $\mathbf{TS_{DE}}$. The deprotonation of a new substrate molecule by the newly formed Zr-OH group enables its binding to the Zr center through a carboxylate oxygen, which occurs concomitantly with the release of a water molecule (see Figure 4, process from **F** to **H**). Finally, the transition from an end-on coordination to a bridging binding mode in the substrate triggers the release of the **2a** product through $\mathbf{TS_{HI}}$ (Figure S9), overcoming an overall barrier of 18.2 kcal mol^{-1} from **F**. Coordination of another GlyGly substrate molecule (shown in purple in Figure 4), poised to act as proton shuttle in the next catalytic cycle, regenerates species **A**, providing a thermodynamic driving force of 16.9 kcal mol^{-1} for the whole reaction.

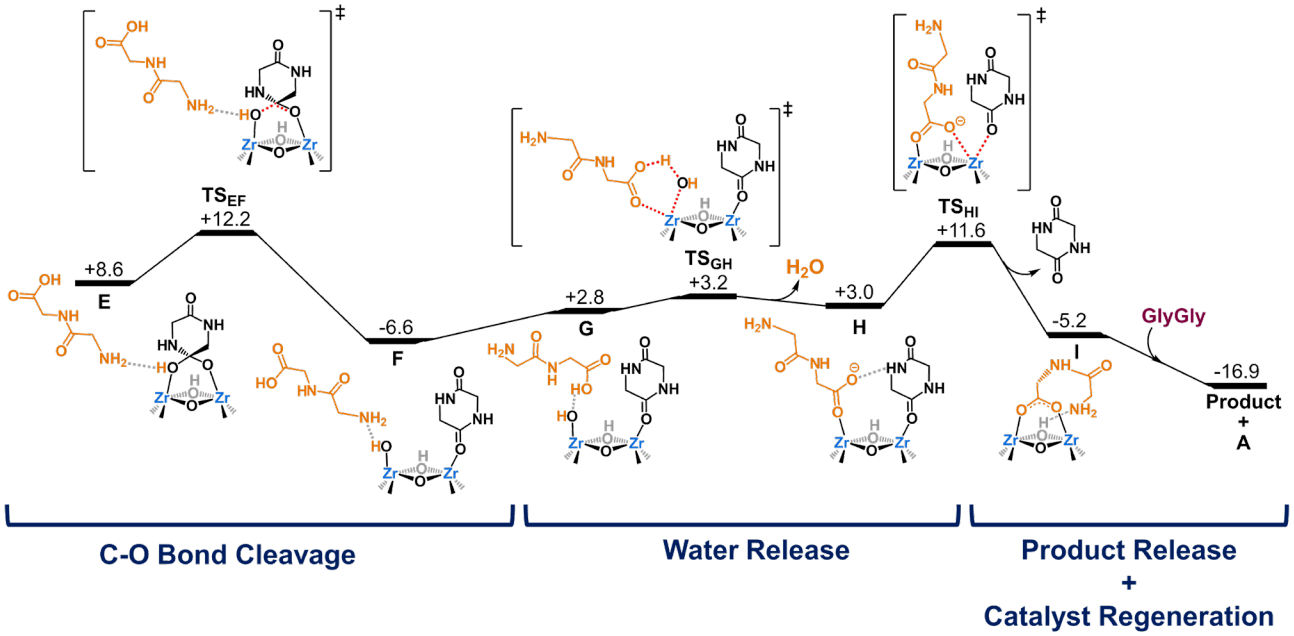

Figure 4. Calculated Gibbs free-energy profile for the C—O bond cleavage, product release and catalyst regeneration steps involved in the cyclization of **GlyGly** catalyzed by **Zr_6-OMc**. All relative free energies are referred to **A** and are displayed in kcal·mol^{-1}.

Differences between peptide and 'regular' amide bond formation by ZrOCs

The mechanism of dipeptide cyclization is similar to the one we reported previously for amide bond formations using ZrOCs as catalysts.[21] However, the dipeptide cyclization reported here required more energy input to afford good product yields than the amide bond formation with 'regular' substrates phenylacetic acid and benzyl amine. Moreover, the solvents had a larger influence for dipeptide substrates than for regular substrates. While the intramolecular peptide bond formation is favored in DMSO at 80°C, this is not the case for the reaction in EtOH. Meanwhile, regular substrates performed well at 80 °C in various solvents, including EtOH and DMSO. Thus, we inspected both mechanisms for differences that could explain the deviations in catalytic performance.

With respect to the calculated mechanism for phenylacetic acid and benzylamine, the dipeptide cyclization presented here has two main differences. First, as summarized in Table 4, GlyGly cyclization promoted by active species **A** requires a higher overall free-energy barrier ($\Delta G_{overall}$) than the 'regular' amide bond formation between phenylacetic acid and benzylamine catalyzed by its analogue **A'**.[21] To clarify the origin of this difference, we examined the individual elementary steps of both mechanisms in detail. The initial nucleophilic attack step was found to be largely insensitive to the nature of the substrate. However, proton abstraction from the ammonium group of the tetrahedral intermediate **B** by the amine of a second substrate molecule (see Figure 3) is favorable in **B'** but unfavorable in **B** (Table 4), being responsible for the higher overall barrier in the dipeptide system. Such a trend is consistent with the pK_a values of the protonated amines: the terminal $-NH_3^+$ group in GlyGly has a pK_a of 8.15[42] compared to 9.43 for benzylamine.[43] Albeit the acidity of the ammonium proton in

the tetrahedral intermediate **B** is also expected to contribute, the lower basicity of the terminal amine in GlyGly compared to benzylamine explains why proton removal is more difficult in the former. Thus, this raises the energy of the resulting intermediate and subsequent species in the reaction profile, in turn increasing the overall barrier.

Table 4. Comparison of the key energetic values (kcal mol^{-1}) of the **Zr_6-Mc** catalyzed intermolecular GlyGly dipeptide cyclization and intermolecular amide bond formation between phenylacetic acid and benzylamine.

Species	$\Delta G_{overall}$	$\Delta G^{\ddagger}$(**A**/**A'**→**TS_{AB}**/**$TS_{AB'}$**)	ΔG (**B**/**B'**→**D**/**D**)	Ref.
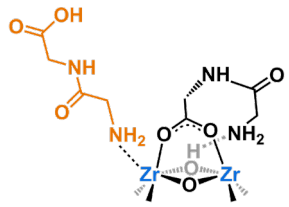 **A**	23.4	+13.7	+5.6	this work
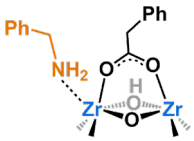 **A'**	18.8	+12.1	-5.9	18[a]

[a] In our previous work, free energies were calculated at T = 70 ºC. All values in this table are scaled to T = 100 ºC for consistency.

Second, the hydrophilicity of cluster's ligand sphere is probably higher for peptide substrates than for phenylacetic acid and benzylamine due to the higher number of hydrogen bond donors and acceptors for dipeptidic substrates. Previously, we observed through molecular dynamics that the hydrophobicity of the ligand shell drives the water molecules away from the active sites, shifting the reaction equilibrium towards amide formation. In contrast, the water generated upon dipeptide intramolecular condensation could remain longer in the vicinity of the active site, interfering with the availability of polar group essential for the key proton transfers in the mechanism. The latter could also be among the causes for the slower reaction observed for the dipeptide cyclization.

Conclusion

In summary, discrete zirconium oxo clusters catalyze the formation of peptide bonds directly from non-activated commercially available substrates. Several 1,2-diketopirazines could be obtained directly from commercially available dipeptides in good to excellent yields using DMSO or EtOH as solvents, without requiring water scavenging unlike many previous reports. In addition, proof-of-concept of intermolecular peptide bond formation

in EtOH from glycine was also demonstrated, showcasing the promising potential of these ZrOCs to be developed further as catalysts for this transformation. Detailed computational mechanistic study revealed the Lewis acidity of ZrOCs plays a crucial role in activating the carboxylate groups and promoting the intramolecular peptide bond formation. Key proton transfers were found to be mediated by a second substrate molecule instead of solvent, which demonstrates that high yields and efficient catalysis can also be achieved in aprotic media. The basicity of the amine group is not only influential in the nucleophilic attack to the carboxylic carbon, but also in the N-to-O proton transfer, which can determine the overall activity of the process. These results provide new mechanistic insights into model Zr-catalyzed systems and lay a strong foundation for the detailed understanding of peptide transformations, supporting the design of future Zr-catalytic systems aimed at achieving high efficiency with more challenging substrates.

Author Information

Corresponding Author

E-mail: francisco.deazambuja@kuleuven.be; tatjana.vogt@kuleuven.be; j.carbo@urv.cat

ORCID

Francisco de Azambuja: 0000-0002-5537-5411

Tatjana N. Parac-Vogt: 0000-0002-6188-3957

Jorge J. Carbó: 0000-0002-3945-6721

Jordi Puiggalí-Jou: 0000-0003-4862-0973

Albert Solé-Daura: 0000-0002-3781-3107

Ismail Y. Kokculer: 0000-0003-1076-6926

Notes The authors declare no competing financial interest.

Associated Content

Supporting Information. Experimental procedures, computational details, supplementary experiments, supplementary figures. This information is available free of charge on …

Acknowledgements

We thank KU Leuven (F.d.A, STG/23/022), Research Foundation Flanders (FWO, F.d.A. 195931/1281921N), the Chinese Scholar Council (CSC, Y.Z. 201804910511), grant PID2021-128128NB-I00 funded by MICIU/AEI/10.13039/501100011033 and by ERDF/EU, the Generalitat de Catalunya (2021SGR00110), The

Scientific and Technological Research Council of Turkey (TUBITAK, I. Y. K. 1059B052001345), and Bilkent University for generous financial support. A.S.-D. acknowledges financial support from the “la Caixa” Foundation (ID 100010434) under the fellowship code LCF/BQ/PI24/12040012, and from the Ramón y Cajal program (RYC2023-043456-I), awarded by the Spanish Ministry of Science, Innovation and Universities.

References

1. Isidro-Llobet, A.; Kenworthy, M. N.; Mukherjee, S.; Kopach, M. E.; Wegner, K.; Gallou, F.; Smith, A. G.; Roschangar, F. Sustainability Challenges in Peptide Synthesis and Purification: From R&D to Production. *J. Org. Chem.* **2019**, *84*, 4615-4628. https://doi.org/10.1021/acs.joc.8b03001

2. Martin, V.; Egelund, P. H. G.; Johansson, H.; Thordal Le Quement, S.; Wojcik, F.; Sejer Pedersen, D. Greening the synthesis of peptide therapeutics: an industrial perspective. *RSC Advances* **2020**, *10*, 42457-42492. http://dx.doi.org/10.1039/D0RA07204D

3. Jadhav, S.; Martin, V.; Egelund, P. H. G.; Johansson Castro, H.; Krüeger, T.; Richner, F.; Thordal Le Quement, S.; Albericio, F.; Dettner, F.; Lechner, C. C.; Schönleber, R.; Pedersen, D. S. Replacing DMF in solid-phase peptide synthesis: Varying the composition of green binary solvent mixtures as a tool to mitigate common side-reactions. *Green Chem.* **2021**. http://dx.doi.org/10.1039/D1GC00604E

4. Commission Regulation (EU) 2021/2030 of 19 November 2021 Amending Annex XVII to Regulation (EC) No 1907/2006 of the European Parliament and of the Council Concerning the Registration, Evaluation, Authorisation and Restriction of Chemicals (REACH) as Regards N,N-Dimethylformamide (Text with EEA Relevance); 2021; Vol. 415. http://data.europa.eu/eli/reg/2021/2030/oj/eng (accessed 2025-02-12).

5. Hannu, T.; Alanko, K.; Keskinen, H. Anaphylaxis and allergic contact urticaria from occupational airborne exposure to HBTU. *Occupational Medicine* **2006**, *56*, 430-433. https://doi.org/10.1093/occmed/kql025

6. Sperry, J. B.; Minteer, C. J.; Tao, J.; Johnson, R.; Duzguner, R.; Hawksworth, M.; Oke, S.; Richardson, P. F.; Barnhart, R.; Bill, D. R.; Giusto, R. A.; Weaver, J. D., III Thermal Stability Assessment of Peptide Coupling Reagents Commonly Used in Pharmaceutical Manufacturing. *Org. Process Res. Dev.* **2018**, *22*, 1262-1275. https://doi.org/10.1021/acs.oprd.8b00193

7. Constable, D. J. C.; Dunn, P. J.; Hayler, J. D.; Humphrey, G. R.; Leazer, J. J. L.; Linderman, R. J.; Lorenz, K.; Manley, J.; Pearlman, B. A.; Wells, A.; Zaks, A.; Zhang, T. Y. Key green chemistry research areas—a perspective from pharmaceutical manufacturers. *Green Chem.* **2007**, *9*, 411-420. http://dx.doi.org/10.1039/B703488C

8. Lundberg, H.; Tinnis, F.; Selander, N.; Adolfsson, H. Catalytic Amide Formation from Non-Activated Carboxylic Acids and Amines. *Chem. Soc. Rev.* **2014**, *43*, 2714-2742. http://dx.doi.org/10.1039/C3CS60345H

9. Todorovic, M.; Perrin, D. M. Recent developments in catalytic amide bond formation. *Peptide Science* **2020**, *112*, e24210. https://doi.org/10.1002/pep2.24210

10. Acosta-Guzmán, P.; Ojeda-Porras, A.; Gamba-Sánchez, D. Contemporary Approaches for Amide Bond Formation. *Adv. Synth. Catal.* **2023**, *n/a*. https://doi.org/10.1002/adsc.202301018

11. Koshizuka, M.; Takahashi, N.; Shimada, N. Organoboron catalysis for direct amide/peptide bond formation. *Chem.*

Commun. **2024**. http://dx.doi.org/10.1039/D4CC02994A

12. Dunetz, J. R.; Magano, J.; Weisenburger, G. A. Large-Scale Applications of Amide Coupling Reagents for the Synthesis of Pharmaceuticals. *Org. Process Res. Dev.* **2016**, *20*, 140-177. https://doi.org/10.1021/op500305s

13. Sabatini, M. T.; Boulton, L. T.; Sneddon, H. F.; Sheppard, T. D. A Green Chemistry Perspective on Catalytic Amide Bond Formation. *Nat. Catal.* **2019**, *2*, 10-17. https://doi.org/10.1038/s41929-018-0211-5

14. Wang, X. Challenges and Outlook for Catalytic Direct Amidation Reactions. *Nat. Catal.* **2019**, *2*, 98-102. https://doi.org/10.1038/s41929-018-0215-1

15. Van den Eynden, D.; Pokratath, R.; De Roo, J. Nonaqueous Chemistry of Group 4 Oxo Clusters and Colloidal Metal Oxide Nanocrystals. *Chem. Rev.* **2022**, *122*, 10538-10572. https://doi.org/10.1021/acs.chemrev.1c01008

16. Vendrame, D.; Bragaggia, G.; Carraro, M.; Gross, S. Metal Oxocluster-Based Organic–Inorganic Hybrid Materials: From Design Principles to Applications. *Chem. Mater.* **2024**, *36*, 9259-9278. https://doi.org/10.1021/acs.chemmater.4c01141

17. Unniram Parambil, A. R.; Pulparayil Mathew, J.; Parammal, M. J.; De Roo, J. M_6O_8 metal oxo clusters: A key structural motif across the periodic table. *Coord. Chem. Rev.* **2026**, *546*, 216967. https://www.sciencedirect.com/science/article/pii/S0010854525005375

18. de Azambuja, F.; Parac-Vogt, T. N. Water-Tolerant and Atom Economical Amide Bond Formation by Metal-Substituted Polyoxometalate Catalysts. *ACS Catal.* **2019**, *9*, 10245-10252. https://doi.org/10.1021/acscatal.9b03415

19. de Azambuja, F.; Lenie, J.; Parac-Vogt, T. N. Homogeneous Metal Catalysts with Inorganic Ligands: Probing Ligand Effects in Lewis Acid Catalyzed Direct Amide Bond Formation. *ACS Catal.* **2021**, *11*, 271-277. https://doi.org/10.1021/acscatal.0c04189

20. de Azambuja, F.; Loosen, A.; Conic, D.; van den Besselaar, M.; Harvey, J. N.; Parac-Vogt, T. N. En Route to a Heterogeneous Catalytic Direct Peptide Bond Formation by Zr-Based Metal–Organic Framework Catalysts. *ACS Catal.* **2021**, *11*, 7647-7658. https://doi.org/10.1021/acscatal.1c01782

21. Zhang, Y.; Puiggalí-Jou, J.; Mullaliu, A.; Solé-Daura, A.; Carbó, J. J.; Parac-Vogt, T. N.; de Azambuja, F. Mechanism Insight into Direct Amidation Catalyzed by Zr Salts: Evidence of Zr Oxo Clusters as Active Species. *Inorg. Chem.* **2024**, *63*, 20347-20360. https://doi.org/10.1021/acs.inorgchem.4c02526

22. Sharma, K.; Sharma, K. K.; Sharma, A.; Jain, R. Peptide-based drug discovery: Current status and recent advances. *Drug Discovery Today* **2023**, *28*, 103464. https://www.sciencedirect.com/science/article/pii/S1359644622004573

23. Nonappa; Ahonen, K.; Lahtinen, M.; Kolehmainen, E. Cyclic dipeptides: catalyst/promoter-free, rapid and environmentally benign cyclization of free amino acids. *Green Chem.* **2011**, *13*, 1203-1209. http://dx.doi.org/10.1039/C1GC15043J

24. Muramatsu, W.; Hattori, T.; Yamamoto, H. Amide bond formation: beyond the dilemma between activation and racemisation. *Chem. Commun.* **2021**, *57*, 6346-6359. http://dx.doi.org/10.1039/D1CC01795K

25. Taussat, A.; de Figueiredo, R. M.; Campagne, J.-M. Direct Catalytic Amidations from Carboxylic Acid and Ester Derivatives: A Review. *Catalysts* **2023**, *13*, 366. https://www.mdpi.com/2073-4344/13/2/366

26. Zhang, Y.; de Azambuja, F.; Parac-Vogt, T. N. The forgotten chemistry of group(IV) metals: A survey on the synthesis, structure, and properties of discrete Zr(IV), Hf(IV), and Ti(IV) oxo clusters. *Coord. Chem. Rev.* **2021**, *438*, 213886. https://doi.org/10.1016/j.ccr.2021.213886

27. Schubert, U. Clusters with a Zr_6O_8 core. *Coord. Chem. Rev.* **2022**, *469*, 214686. https://www.sciencedirect.com/science/article/pii/S0010854522002818

28. Lundberg, H.; Tinnis, F.; Adolfsson, H. Direct Amide Coupling of Non-activated Carboxylic Acids and Amines Catalysed by Zirconium(IV) Chloride. *Chem. Eur. J.* **2012**, *18*, 3822-3826. https://doi.org/10.1002/chem.201104055

29. Li, N.; Wang, L.; Zhang, L.; Zhao, W.; Qiao, J.; Xu, X.; Liang, Z. Air-stable Bis(pentamethylcyclopentadienyl) Zirconium Perfluorooctanesulfonate as an Efficient and Recyclable Catalyst for the Synthesis of N-substituted Amides. *ChemCatChem* **2018**, *10*, 3532-3538. https://doi.org/10.1002/cctc.201800590

30. Zhang, Y.; de Azambuja, F.; Parac-Vogt, T. N. Zirconium oxo clusters as discrete molecular catalysts for the direct amide bond formation. *Catal. Sci. Technol.* **2022**, *12*, 3190-3201. http://dx.doi.org/10.1039/D2CY00421F

31. Zhang, Y.; Kokculer, I. Y.; de Azambuja, F.; Parac-Vogt, T. N. Dynamic Environment at the Zr_6 Oxo Cluster Surface Is Key for the Catalytic Formation of Amide Bonds. *Catal. Sci. Technol.* **2023**, *13*, 100-110. http://dx.doi.org/10.1039/D2CY01706G

32. Kickelbick, G.; Wiede, P.; Schubert, U. Variations in capping the $Zr_6O_4(OH)_4$ cluster core: X-ray structure analyses of $[Zr_6(OH)_4O_4(OOC–CH=CH_2)_{10}]_2(\mu\text{-}OOC–CH=CH_2)_4$ and $Zr_6(OH)_4O_4(OOCR)_{12}(PrOH)$ (R=Ph, $CMe=CH_2$). *Inorg. Chim. Acta* **1999**, *284*, 1-7. https://doi.org/10.1016/S0020-1693(98)00251-5

33. Kogler, F. R.; Jupa, M.; Puchberger, M.; Schubert, U. Control of the ratio of functional and non-functional ligands in clusters of the type $Zr_6O_4(OH)_4(carboxylate)_{12}$ for their use as building blocks for inorganic–organic hybrid polymers. *J. Mater. Chem.* **2004**, *14*, 3133-3138. http://dx.doi.org/10.1039/B405769D

34. Walther, P.; Puchberger, M.; Kogler, F. R.; Schwarz, K.; Schubert, U. Ligand dynamics on the surface of zirconium oxo clusters. *Physical Chemistry Chemical Physics* **2009**, *11*, 3640-3647. http://dx.doi.org/10.1039/B820731C

35. Chiu, C.-C.; Shieh, F.-K.; Tsai, H.-H. G. Ligand Exchange in the Synthesis of Metal–Organic Frameworks Occurs Through Acid-Catalyzed Associative Substitution. *Inorg. Chem.* **2019**, *58*, 14457-14466. https://doi.org/10.1021/acs.inorgchem.9b01947

36. Schubert, U. Surface chemistry of carboxylato-substituted metal oxo clusters – Model systems for nanoparticles. *Coord. Chem. Rev.* **2017**, *350*, 61-67. http://www.sciencedirect.com/science/article/pii/S0010854517302382

37. Murali, M.; Bijani, C.; Daran, J.-C.; Manoury, E.; Poli, R. Acetate exchange mechanism on a Zr12 oxo hydroxo cluster: relevance for reshaping Zr–carboxylate coordination adaptable networks. *Chem. Sci.* **2023**, *14*, 8152-8163. http://dx.doi.org/10.1039/D3SC02204H

38. Yang, D.; Ortuño, M. A.; Bernales, V.; Cramer, C. J.; Gagliardi, L.; Gates, B. C. Structure and Dynamics of Zr_6O_8 Metal–Organic Framework Node Surfaces Probed with Ethanol Dehydration as a Catalytic Test Reaction. *J. Am. Chem. Soc.* **2018**, *140*, 3751-3759. https://doi.org/10.1021/jacs.7b13330

39. Xia, P.; Wang, C.; Qi, C. Theoretical Study on the Cyclization Mechanism of Dipeptides. *Chin. J. Chem* . **2013**, *31*, 813-818. https://doi.org/10.1002/cjoc.201300035

40. Schindele, C.; Houk, K. N.; Mayr, H. Relationships between Carbocation Stabilities and Electrophilic Reactivity Parameters, E: Quantum Mechanical Studies of Benzhydryl Cation Structures and Stabilities. *J. Am. Chem. Soc.* **2002**, *124*, 11208-11214. https://doi.org/10.1021/ja020617b

41. Wang, C.; Fu, Y.; Guo, Q.-X.; Liu, L. First-Principles Prediction of Nucleophilicity Parameters for π Nucleophiles: Implications for Mechanistic Origin of Mayr's Equation. *Chem. Eur. J.* **2010**, *16*, 2586-2598. https://doi.org/10.1002/chem.200902484

42. Sigel, H. Ternary complexes in solution. XXIII. Influence of alkyl side chains on the stability of binary and ternary copper(II)-dipeptide complexes. *Inorg. Chem.* **1975**, *14*, 1535-1540. https://doi.org/10.1021/ic50149a018

43. Bunting, J. W.; Stefanidis, D. A systematic entropy relationship for the general-base catalysis of the deprotonation of a carbon acid. A quantitative probe of transition-state solvation. *J. Am. Chem. Soc.* **1990**, *112*, 779-786. https://doi.org/10.1021/ja00158a043